Magnetic multipole induced zero-rotation frequency bounce-resonant loss in a Penning–Malmberg trap used for antihydrogen trapping

G. B. Andresen,[1] W. Bertsche,[2] C. C. Bray,[3] E. Butler,[2] C. L. Cesar,[4] S. Chapman,[3] M. Charlton,[2] J. Fajans,[3] M. C. Fujiwara,[5] D. R. Gill,[5] W. N. Hardy,[6] R. S. Hayano,[7] M. E. Hayden,[8] A. J. Humphries,[2] R. Hydomako,[9] L. V. Jørgensen,[2] S. J. Kerrigan,[2] J. Keller,[3] L. Kurchaninov,[5] R. Lambo,[4] N. Madsen,[2] P. Nolan,[10] K. Olchanski,[5] A. Olin,[5] A. Povilus,[3] P. Pusa,[10] F. Robicheaux,[11] E. Sarid,[12] S. Seif El Nasr,[6] D. M. Silveira,[7,13] J. W. Storey,[5] R. I. Thompson,[9] D. P. van der Werf,[2] J. S. Wurtele,[3] and Y. Yamazaki[13] (ALPHA Collaboration)

[1]*Department of Physics and Astronomy, Aarhus University, DK-8000 Aarhus C, Denmark*
[2]*Department of Physics, Swansea University, Swansea SA2 8PP, United Kingdom*
[3]*Department of Physics, University of California at Berkeley, Berkeley, California 94720-7300, USA*
[4]*Instituto de Física, Universidade Federal do Rio de Janeiro, Rio de Janeiro 21941-972, Brazil*
[5]*TRIUMF, 4004 Wesbrook Mall, Vancouver, British Columbia V6T 2A3, Canada*
[6]*Department of Physics and Astronomy, University of British Columbia, Vancouver, British Columbia V6T 1Z4, Canada*
[7]*Department of Physics, University of Tokyo, Tokyo 113-0033, Japan*
[8]*Department of Physics, Simon Fraser University, Burnaby, British Columbia V5A 1S6, Canada*
[9]*Department of Physics and Astronomy, University of Calgary, Calgary, Alberta T2N 1N4, Canada*
[10]*Department of Physics, University of Liverpool, Liverpool L69 7ZE, United Kingdom*
[11]*Department of Physics, Auburn University, Auburn, Alabama 36849-5311, USA*
[12]*Department of Physics, NRCN-Nuclear Research Center Negev, Beer Sheva IL-84190, Israel*
[13]*Atomic Physics Laboratory, RIKEN, Saitama 351-0198, Japan*

(Received 21 May 2009; accepted 15 October 2009; published online 30 October 2009)

In many antihydrogen trapping schemes, antiprotons held in a short-well Penning–Malmberg trap are released into a longer well. This process necessarily causes the bounce-averaged rotation frequency $\bar{\Omega}_r$ of the antiprotons around the trap axis to pass through zero. In the presence of a transverse magnetic multipole, experiments and simulations show that many antiprotons (over 30% in some cases) can be lost to a hitherto unidentified bounce-resonant process when $\bar{\Omega}_r$ is close to zero. © *2009 American Institute of Physics*. [doi:10.1063/1.3258840]

Experiments[1,2] designed to create and trap antihydrogen ($\bar{H}$) confine antiprotons ($\bar{p}$'s) in Penning–Malmberg traps (see Fig. 1). Such traps use an electrostatic well to confine the $\bar{p}$'s axially, and a solenoidal field to confine them radially. To make $\bar{H}$, the $\bar{p}$'s are often first excited so that they have a hollow phase space distribution,[3] and then mixed with positrons (e^+'s) confined in a nearby electrostatic well of the opposite polarity.[3,4] Mixing is commonly accomplished by manipulating the $\bar{p}$ electrostatic well so that the $\bar{p}$'s escape from their initial well into a longer "double" well that contains the e^+'s. Because of $\mathbf{E}\times\mathbf{B}$ drifts from the confinement fields, the $\bar{p}$'s rotate around the trap axis. When the $\bar{p}$ energy is such that the $\bar{p}$'s can almost escape into the longer well, their rotation direction reverses near the escape-side well wall, and their bounce-averaged rotation frequency $\bar{\Omega}_r$ will pass through zero. At this zero-rotation frequency bounce resonance, we observe a hitherto unidentified process that transports $\bar{p}$'s radially into the trap wall when the trap also employs a magnetic multipole. (The multipole's function is to confine $\bar{H}$ produced during the mixing process.)

Bounce-resonant loss processes have long been studied in non-neutral,[5,6] neutral,[7] planetary, and solar plasmas,[8] and are thought, for instance, to play a major role in loss in mirror machines.[7] The unambiguous identification of bounce-resonant losses has proved difficult, however.

The bounce-resonant loss may seriously complicate efforts to trap $\bar{H}$. The most efficient $\bar{H}$ formation schemes now known[3,4,9] are all potentially subject to this loss. Indeed, in the most recent experiments,[10,11] which have attempted to make relatively cold $\bar{H}$ by slowing the movement of the electrostatic potentials, the likelihood of this loss is enhanced. A large fraction (over 20%) of the $\bar{p}$'s were lost in the experiments described here (see Fig. 2). In other experiments we observed losses of 30%; this fraction could be even higher under some experimental conditions.

There are several other processes which can cause $\bar{p}$ loss during mixing, including the loss of untrapped $\bar{H}$ atoms, and the ballistic[12,13] loss of $\bar{p}$'s directly and from reionized $\bar{H}$. The characteristics of the bounce-resonant loss have a clear experimental signature which distinguishes it from the others. (1) It occurs only with a multipole field: an octupole, in our case. (2) Loss occurs only when the potentials are changed such that the $\bar{p}$ orbits expand from a short well into a long well. Over a broad range, the loss primarily depends on the potential change itself, and only weakly on the rate at which the potential change is effected. For example, in Fig. 2, the loss increases by only a factor of 1.6 when the ramp time is increased from 16 to 320 s. The loss is dramatically larger than the loss which occurs for static potentials. (3) The line integrated radial profile, which begins as a ~1 mm ra-

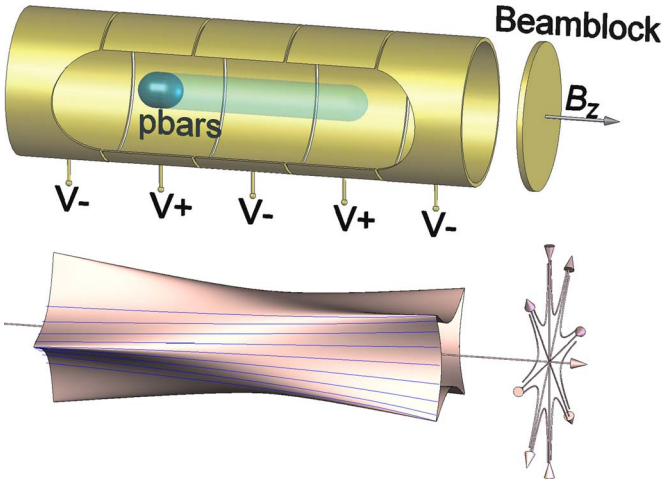

FIG. 1. (Color online) Top: simplified trap schematic (not to scale) showing five electrodes and the voltages impressed on them to make a double well potential, and the initial (solid) and final (transparent) $\bar{p}$ locations. Bottom: magnetic field lines and surfaces from the combined solenoidal and octupolar fields. The surfaces are formed by tracing the field lines emanating from a circular locus of points.

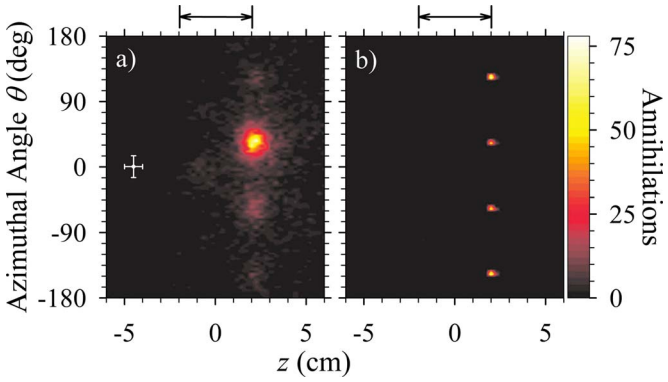

FIG. 3. (Color online) (a) Experimentally determined z-θ positions of the annihilations (Ref. 14) from resonant loss. The arrows mark the location of the initial short well. Also shown is the one-sigma position reconstruction error. (b) "Annihilation" locations found in a similar well by our Lorentz simulation. In both cases, the annihilations occur at the cusps of the octupole field (see Fig. 1) on the escape side of the well only. The annihilations in (a) are not as symmetrically distributed in θ as in (b); numeric simulations suggest that this may be due to field and alignment errors in the experiment.

dius near Gaussian with a long tail, does not change substantially even after many $\bar{p}$'s have been lost; those $\bar{p}$'s not lost do not appear to undergo significant radial transport. (4) Lost $\bar{p}$'s annihilate within the axial confines of the original short well, implying that they are lost radially before they escape axially into the long well. Most annihilate in one of the escape-side cusps of the magnetic surfaces (see Figs. 1 and 3).

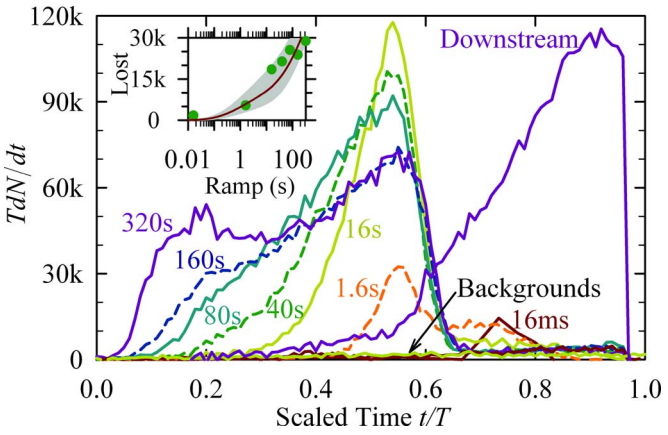

FIG. 2. (Color online) Resonant loss rates (TdN/dt) for the listed potential ramp times T, all scaled to a common time axis (t/T). The "downstream" curve plots the rate (scaled down by a factor of 3) at which $\bar{p}$'s escape over the central potential barrier and annihilate on the distant beamblock (see Fig. 1). Downstream losses are readily distinguished from the resonant losses by our position sensitive annihilation detector; resonant losses occur at one end of the original well and are radial losses (see Fig. 3), while downstream losses are axial and occur at or near the beamblock far outside the octupole. At the end of the ramp, all $\bar{p}$'s are either lost by the resonant process or by escaping over the central barrier. Also plotted are two indistinguishable backgrounds: a 160 s ramp with the octupole off and a 160 s hold with the octupole on, but with a static potential. Inset: total ($\int_0^T dt dN/dt$) number of $\bar{p}$'s lost resonantly as a function of ramp time; the line and band plot the predicted loss, as discussed in the text.

In our as yet unsuccessful attempts to demonstrate $\bar{H}$ trapping, we use a complete double well potential; the downstream wall (the rightmost V− in Fig. 1) confines $\bar{p}$'s which escape over the central barrier (the center V−). This could allow secondary processes to cause loss in the now longer well. Experiments (not shown) similar to those in Fig. 3 suggest that this is not the case, but, to eliminate the possibility, the experiments reported here were done with the downstream wall removed. Any $\bar{p}$'s that escape over the central barrier immediately annihilate on a downstream beamblock (see Figs. 1 and 2).

We have studied the loss process using a Lorentz model which propagates $\bar{p}$'s numerically using the full Lorentz equations of motion in the exact electrostatic potential. It reproduces the experimental observations including the signatures 1–4 above, but the loss physics is more clearly elucidated in a reduced model that propagates $\bar{p}$'s using guiding-centerlike equations. The results from these models are qualitatively and quantitatively similar.

The reduced equations of motion in cylindrical coordinates (r,θ,z) are

$$\frac{dr}{dt} = v_r(z) = \frac{B_r}{|B|} v_s, \tag{1}$$

$$\frac{d\theta}{dt} = \frac{1}{r}\left(\frac{B_\theta}{|B|} v_s - \frac{E_r B_z}{|B|^2}\right), \tag{2}$$

$$\frac{dz}{dt} = \frac{B_z}{|B|} v_s, \tag{3}$$

$$\frac{dv_s}{dt} = -\frac{e}{m_p |B|}(B_z E_z + B_r E_r), \tag{4}$$

where v_s is the velocity along the magnetic field, and e and m_p are the $\bar{p}$ charge and mass. The fields B_r and B_θ are defined by our complete magnetic field,

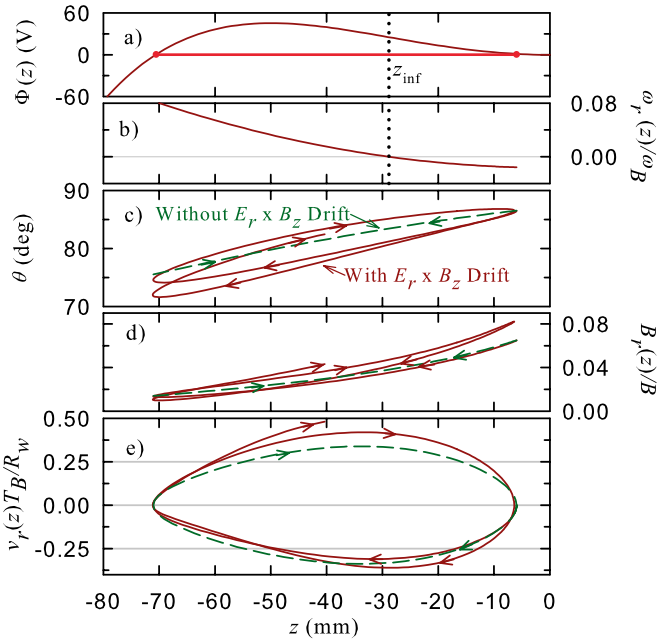

FIG. 4. (Color online) Resonant loss physics. The individual graphs are explained in the text.

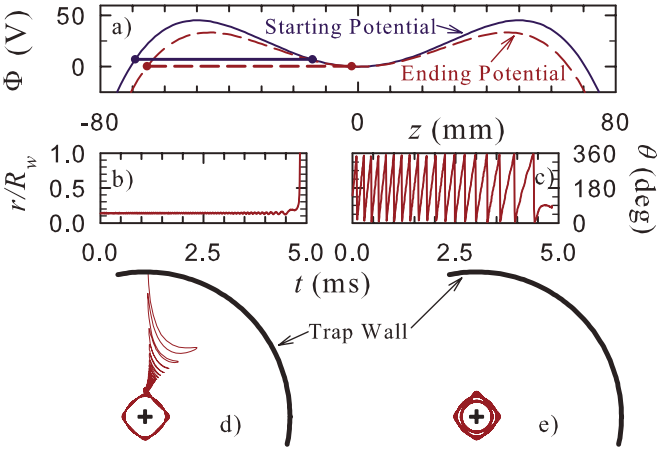

FIG. 5. (Color online) Antiproton trajectories calculated in the reduced model. (a) The potentials and orbit extents at the beginning and end of the simulation. (b) The normalized radius as a function of time. (c) The angle θ as a function of time. Note how the rotation frequency $d\theta/dt$ gradually decreases as the resonance is approached, and the $\bar{p}$ are abruptly lost when the rotation stalls. (d) The x-y projection of the orbit of the $\bar{p}$. Plot (e) shows a second simulation with initial conditions slightly different than the initial conditions used for (a)–(d); the only change is in the initial angle. This small change causes the $\bar{p}$ to escape over the central barrier into the longer double well; this $\bar{p}$ is not lost radially.

$$\mathbf{B} = B_w(r/R_w)^3[\cos(4\theta)\hat{\mathbf{r}} - \sin(4\theta)\hat{\boldsymbol{\theta}}] + B_z\hat{\mathbf{z}}, \tag{5}$$

where $R_w=22.27$ mm is the trap wall radius, $B_w=1.4$ T is the magnitude of the octupole field at the wall, and $B_z=1$ T is the solenoidal field. Equation (1), the first term in Eq. (2), and Eq. (3) propagate the $\bar{p}$'s along the magnetic field lines. The second term in Eq. (2) is the $E_r\times B_z$ drift, which causes the $\bar{p}$'s to rotate around the trap axis, and Eq. (4) is the force equation along the magnetic field. All other drifts are ignored. The electric fields E_r and E_z are defined by $-\nabla\Phi$, where Φ is the double well potential in this model,

$$\Phi(r,z) = V_0(az^2 - 0.5ar^2 - z^4 - 0.375r^4 + 3r^2z^2). \tag{6}$$

The constant V_0 and the variable a determine the depth and width of the well. As time progresses, a diminishes slowly following $a=a_0(1-\Gamma t)$, where a_0 and Γ are constant, so that the central barrier becomes ever lower. (The values $a=5\times10^5$ mm^2 and $V_0=7.5\times10^{-10}$ V/mm^4 produce a well similar to the experimental wells.)

The resonant loss physics is illustrated in Fig. 4. Figure 4(a) graphs the well potential $\Phi(r,z)$ (dark red curve) for typical parameters, and bounce limits (red horizontal line) for a $\bar{p}$ that is near to escaping over the right side well barrier. (All curves in Fig. 4 are computed at $r=0$.) Figure 4(b) graphs the local rotation frequency $\omega_r(z)$ induced by the $E_r\times B_z$ drift, normalized by the bounce frequency $\omega_B=2\pi/T_B$. At the inflection point in the potential, indicated by the dotted vertical lines in Figs. 4(a) and 4(b), the E_r field, and, consequently, the rotation, reverse direction. The net rotation in one complete $\hat{\mathbf{z}}$-bounce cycle is found by integrating over the bounce orbit. At the resonant energy, the oppositely directed rotations on either side of the inflection point cancel, leaving no net rotation, i.e., $\bar{\Omega}_r=0$.

If there were no $E_r\times B_z$ drifts, the $\bar{p}$'s would simply bounce back and forth along an octupole field line, as shown by the green dashed trajectory in Fig. 4(c). When the local $E_r\times B_z$ drifts are included, the orbit, as shown by the dark red solid trajectory, is a nearly closed ellipse when $\bar{\Omega}_r$ is near zero. [1.75 bounce cycles are plotted for the trajectories in Figs. 4(c)–4(e).] Figure 4(d) shows the normalized radial component B_r of the multipole field along the trajectories in Fig. 4(c). This field component causes the $\bar{p}$'s to move radially. Without any $E_r\times B_z$ drifts, the local velocity $v_r(z)$ [Eq. (1)] of these radial excursions, shown in Fig. 4(e), cancels when integrated over a complete bounce cycle. But with the local $E_r\times B_z$ drifts, the velocity does not cancel, as suggested by the positive bias of the curves, and there is a net outward drift $\Delta r=\oint dz v_r(z)/v(z)$. If $\bar{\Omega}_r$ stays near zero for long enough, and if the $\bar{p}$'s arrive at the resonant energy with an appropriate phase θ, repeated bounce cycles can quickly transport the $\bar{p}$'s to the trap wall. Figure 5 shows two typical trajectories, one with a phase that leads to loss, and the other with a phase that does not.

The $E_r\times B_z$ rotational frequency is a function of radius, and this, seemingly, would cause an initially resonant $\bar{p}$ to lose resonance as it progresses outward. However, there is an additional rotational drift, caused by a mechanism very similar to the mechanism outlined in Fig. 4, but acting with the B_θ octupole field instead of the B_r field, which can feedback stabilize the resonance condition. Simulations show that this feedback mechanism is powerful enough to maintain the resonance for long initial wells, but is insufficient for short initial wells where the dependence of the $E_r\times B_z$ rotation frequency on the radius is stronger. In the Lorentz model, the

transition between stable and unstable orbits is at ~50 mm for typical experimental parameters. In the apparatus, we observe that $\bar{p}$'s held in ~70 mm initial wells are unstable, while $\bar{p}$'s held in ~44 mm wells are stable.

The ramping potential is intrinsic to the loss process because it ensures that the $\bar{p}$'s will progress through the resonant energy. However, the ramping makes it difficult to predict exactly which initial conditions result in resonant loss, and which initial conditions are stable. As a general rule, particles near the $r=0$ axis are stable, and particles far from the axis are lost resonantly, but at intermediate radii, stability depends sensitively on the initial conditions. Nonetheless, using the reduced model, it is possible to derive a scaling law that predicts the loss radius threshold as a function of the ramp rate Γ. The derivation is too lengthy to be included here, but we find that the loss threshold radius is proportional to $(B_z/B_w)^{1/3}\Gamma^{-1/6}$. The line in the Fig. 2 inset plots this relation, properly convolved with the measured radial distribution function, with a proportionality constant fit to the data. This curve is sensitive to the details of the long tail of the radial $\bar{p}$ distribution, something we cannot measure with precision. The banded region shows the results of the scaling with the tail distribution doubled and halved.

We note that the $\bar{\Omega}_r=0$ loss mechanism described here is quite different from the bounce-resonant loss mechanism previously identified[6] for nonzero $\bar{\Omega}_r$ in a static trap, in which loss occurs when the $\bar{p}$'s rotate around the trap axis by a fixed angle in one round trip: 180° in a quadrupole or 90° in an octupole. When this condition is satisfied the $\bar{p}$'s can travel on field lines that direct them monotonically outward as they bounce axially. In the mechanism discussed in this Letter, the $\bar{p}$'s travel on field lines that cause them to oscillate radially as they bounce; net radial motion occurs because of asymmetries in their radial oscillations. We also note that we have here discussed a single particle mechanism; we are currently studying the influence of collective phenomena on the instability.

In conclusion, we have discovered a new bounce-resonant loss mechanism in an octupole that occurs when $\bar{p}$'s are released from a short well into a long well. This operation is common in mixing procedures used to synthesize $\bar{H}$. This mechanism can cause $\bar{p}$'s to be lost over a wide range of parameters, including $\bar{p}$'s that are well within the radii previously identified as safe.[12,13] Loss only occurs when the $\bar{p}$'s pass through the $\bar{\Omega}_r=0$ resonance slowly, but such changes are now common in these mixing cycles,[10,11] as slow changes are believed to decrease the energy and increase the trapping probability of the resulting $\bar{H}$.

While we have here explored loss in an octupole magnet, this type of loss will occur with any multipole magnet. For lower order multipoles, simulations show that this mechanism is more powerful, as the near-axis fields are larger in lower order multipoles.[15]

This work was supported by CNPq, FINEP (Brazil), ISF (Israel), MEXT (Japan), FNU (Denmark), NSERC, NRC/TRIUMF (Canada), DOE (USA), and EPSRC and the Leverhulme Trust (U.K.).

[1] G. Andresen, W. Bertsche, A. Boston, P. D. Bowe, C. L. Cesar, S. Chapman, M. Charlton, M. Chartier, A. Deutsch, J. Fajans, M. C. Fujiwara, R. Funakoshi, D. R. Gill, K. Gomberoff, J. S. Hangst, R. S. Hayano, R. Hydomako, M. J. Jenkins, L. V. Jørgensen, L. Kurchaninov, N. Madsen, P. Nolan, K. Olchanski, A. Olin, A. Povilus, F. Robicheaux, E. Sarid, D. M. Silveira, J. W. Storey, H. H. Telle, R. I. Thompson, D. P. van der Werf, J. S. Wurtele, and Y. Yamazaki, Phys. Rev. Lett. **98**, 023402 (2007).
[2] G. Gabrielse, P. Larochelle, D. L. Sage, B. Levitt, W. S. Kolthammer, I. Kuljanishvili, R. McConnell, J. Wrubel, F. M. Esser, H. Glückler, D. Grzonka, G. Hansen, S. Martin, W. Oelert, J. Schillings, M. Schmitt, T. Sefzick, H. Soltner, Z. Zhang, D. Comeau, M. C. George, E. A. Hessels, C. H. Storry, M. Weel, A. Speck, F. Nillius, J. Walz, and T. W. Hänsch, Phys. Rev. Lett. **98**, 113002 (2007).
[3] M. Amoretti, C. Amsler, G. Bonomi, A. Bouchta, P. Bowe, C. Carraro, C. Cesar, M. Charlton, M. J. T. Collier, M. Doser, V. Filippini, K. S. Fine, A. Fontana, M. C. Fujiwara, R. Funakoshi, P. Genova, J. S. Hangst, R. S. Hayano, M. H. Holzscheiter, L. V. Jørgensen, V. Lagomarsino, R. Landua, D. Lindelöf, E. Lodi Rizzini, M. Macrì, N. Madsen, G. Manuzio, M. Marchesotti, P. Montagna, H. Pruys, C. Regenfus, P. Riedler, J. Rochet, A. Rotondi, G. Rouleau, G. Testera, A. Variola, T. L. Watson, and D. P. van der Werf, Nature (London) **419**, 456 (2002).
[4] G. Gabrielse, N. S. Bowden, P. Oxley, A. Speck, C. H. Storry, J. N. Tan, M. Wessels, D. Grzonka, W. Oelert, G. Schepers, T. Sefzick, J. Walz, H. Pittner, T. W. Hänsch, and E. A. Hessels, Phys. Rev. Lett. **89**, 213401 (2002).
[5] D. Eggleston, in *Non-Neutral Plasma Physics III*, edited by J. Bollinger, R. Spencer, and R. Davidson (AIP, New York, 1999), Vol. 498, p. 241.
[6] E. P. Gilson and J. Fajans, Phys. Rev. Lett. **90**, 015001 (2003).
[7] D. Ryutov and G. Stupakov, JETP Lett. **26**, 174 (1977).
[8] B. Meerson, P. Sasorov, and A. Stepanov, Sol. Phys. **58**, 165 (1978).
[9] M. Amoretti, C. Amsler, G. Bazzano, G. Bonomi, A. Bouchta, P. Bowe, C. Carraro, C. Cesar, M. Charlton, M. Doser, V. Filippini, A. Fontana, M. C. Fujiwara, R. Funakoshi, P. Genova, J. S. Hangst, R. S. Hayano, L. V. Jørgensen, V. Lagomarsino, R. Landua, D. Lindelöf, E. Lodi Rizzini, M. Macri, N. Madsen, G. Manuzio, M. Marchesotti, P. Montagna, H. Pruys, C. Regenfus, P. Riedler, A. Rotondi, G. Rouleau, G. Testera, A. Variola, and D. P. van der Werf, Phys. Lett. B **578**, 23 (2004).
[10] G. Gabrielse, P. Larochelle, D. L. Sage, B. Levitt, W. S. Kolthammer, R. McConnell, P. Richerme, J. Wrubel, A. Speck, M. C. George, D. Grzonka, W. Oelert, T. Sefzick, Z. Zhang, A. Carew, D. Comeau, E. A. Hessels, C. H. Storry, M. Weel, and J. Walz, Phys. Rev. Lett. **100**, 113001 (2008).
[11] G. B. Andresen, W. Bertsche, P. D. Bowe, C. C. Bray, E. Butler, C. L. Cesar, S. Chapman, M. Charlton, J. Fajans, M. C. Fujiwara, R. Funakoshi, D. R. Gill, J. S. Hangst, W. N. Hardy, R. S. Hayano, M. E. Hayden, A. J. Humphries, R. Hydomako, M. J. Jenkins, L. V. Jorgensen, L. Kurchaninov, R. Lambo, N. Madsen, P. Nolan, K. Olchanski, A. Olin, R. D. Page, A. Povilus, P. Pusa, F. Robicheaux, E. Sarid, S. Seif El Nasr, D. M. Silveira, J. W. Storey, R. I. Thompson, D. P. van der Werf, J. S. Wurtele, and Y. Yamazaki, AIP Conf. Proc. **1037**, 241 (2008).
[12] J. Fajans, W. Bertsche, K. Burke, S. F. Chapman, and D. P. van der Werf, Phys. Rev. Lett. **95**, 155001 (2005).
[13] J. Fajans, N. Madsen, and F. Robicheaux, Phys. Plasmas **15**, 032108 (2008).
[14] M. C. Fujiwara, G. B. Andresen, W. Bertsche, P. D. Bowe, C. C. Bray, E. Butler, C. L. Cesar, S. Chapman, M. Charlton, J. Fajans, R. Funakoshi, D. R. Gill, J. S. Hangst, W. N. Hardy, R. S. Hayano, M. E. Hayden, A. J. Humphries, R. Hydomako, M. J. Jenkins, L. V. Jorgensen, L. Kurchaninov, W. Lai, R. Lambo, N. Madsen, P. Nolan, K. Olchanski, A. Olin, A. Povilus, P. Pusa, F. Robicheaux, E. Sarid, S. Seif El Nasr, D. M. Silveira, J. W. Storey, R. I. Thompson, D. P. van der Werf, L. Wasilenko, J. S. Wurtele, and Y. Yamazaki, AIP Conf. Proc. **1037**, 208 (2008).
[15] J. Fajans and A. Schmidt, Nucl. Instrum. Methods Phys. Res. A **521**, 318 (2004).